

# The superconducting high-resolution soft X-ray spectrometer at the advanced biological and environmental X-ray facility

S. Friedrich<sup>a,b,\*</sup>, O.B. Drury<sup>a,b,c</sup>, S.J. George<sup>b</sup>, S.P. Cramer<sup>b,c</sup>

<sup>a</sup>Advanced Detector Group, Lawrence Livermore National Laboratory, 7000 East Avenue, L-188, Livermore, CA 94550, USA

<sup>b</sup>Advanced Biological and Environmental X-ray Facility, Lawrence Berkeley National Laboratory, 1 Cyclotron Road, MS 6-2100, Berkeley, CA 94720, USA

<sup>c</sup>Biophysics Group, University of California, 1 Shields Avenue, EU-III, Davis, CA 95616, USA

Available online 14 August 2007

## Abstract

We have built a 36-pixel superconducting tunnel junction X-ray spectrometer for chemical analysis of dilute samples in the soft X-ray band. It offers an energy resolution of  $\sim 10\text{--}20$  eV FWHM below 1 keV, a solid angle coverage of  $\sim 10^{-3}$ , and can be operated at total rates of up to  $\sim 10^6$  counts/s. Here, we describe the spectrometer performance in speciation measurements by fluorescence-detected X-ray absorption spectroscopy at the Advanced Biological and Environmental X-ray facility at the ALS synchrotron.

Published by Elsevier B.V.

## 1. Introduction

Superconducting tunnel junction (STJ) solid-state detectors are being developed for soft X-ray spectroscopy at the synchrotron because they combine the high energy resolution of low-temperature operation with the high count rate capabilities of athermal detectors [1,2]. STJs consist of two superconducting films separated by a thin insulating tunnel barrier. X-ray absorption in one of the films excites excess charges above the superconducting energy gap  $\Delta$  in proportion to the X-ray energy. As these charges tunnel across the barrier, they produce a temporary increase in current that can be read out with a preamplifier at room temperature. Since the energy gap  $\Delta$  (meV) is 3 orders of magnitude smaller in superconductors than in semiconductors, STJ detectors offer a factor  $\sqrt{1000\sim 30}$  improvement in energy resolution over conventional Si(Li) or Ge detectors. Their maximum count rate is set by the  $\sim \mu\text{s}$  lifetime of the excess charges to several 10,000 counts/s per pixel. These characteristics make STJ detectors well suited for chemical analysis of dilute samples by fluorescence detected X-ray absorption spectroscopy (XAS) below

$\sim 1$  keV where characteristic X-ray emission lines are closely spaced and fluorescence yields are low.

We have built a high-resolution STJ spectrometer that has been in use at the Advanced Biological and Environmental X-ray facility (ABEX) at the ALS synchrotron in Berkeley since 2001. It is primarily used for XAS on K-edges of first row elements, L-edges of first row transition metals and M-edges of rare earth elements. Here, we describe the performance of the instrument after recent upgrades and discuss typical applications.

## 2. Superconducting spectrometer design

The STJ spectrometer at the ABEX facility is based on four  $3 \times 3$  arrays of Nb(165 nm)–Al(50 nm)–AlO<sub>x</sub>–Al(50 nm)–Nb(265 nm) tunnel junctions. The 165-nm-thick top Nb film serves as the primary, and the 265-nm-thick bottom Nb film as the secondary X-ray absorber. This design increases the quantum efficiency of the instrument, especially at energies above 1 keV where the top Nb film is partially transparent, albeit at the expense of a line-splitting artifact since the signal height is  $\sim 5\%$  higher for bottom layer than for top layer events [2].

The STJ arrays are operated in a cryostat that uses liquid N<sub>2</sub> and He for pre-cooling to 77 and 4.2 K, respectively, and a two-stage adiabatic demagnetization refrigerator (ADR) to cool the detectors to their operating temperature

\*Corresponding author. Advanced Detector Group, Lawrence Livermore National Laboratory, 7000 East Avenue, L-188, Livermore, CA 94550, USA. Tel.: +1 925 423 1527; fax: +1 925 424 5512.

E-mail address: [Friedrich1@llnl.gov](mailto:Friedrich1@llnl.gov) (S. Friedrich).

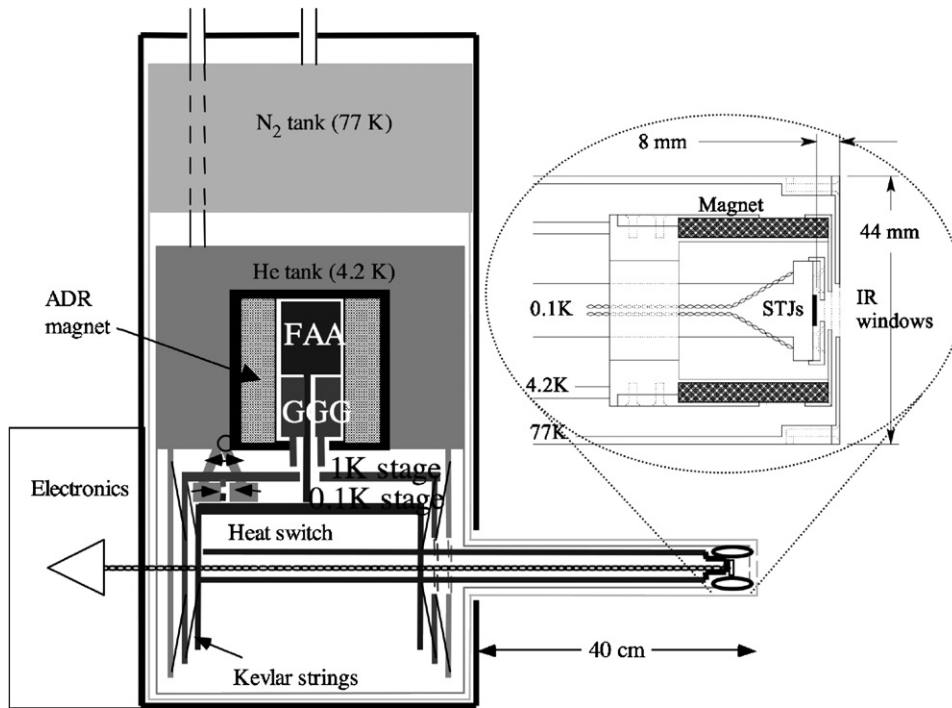


Fig. 1. Schematic cross-section of the superconducting spectrometer. The inset show the end of the cold finger with the sensor arrays held behind three IR blocking window.

at  $\sim 0.1$  K [3]. The superconducting detectors are operated at the end of a 40-cm-long cold finger behind infrared blocking windows at 77, 4.2 and 0.1 K. The cold finger has recently been redesigned to reduce the distance between the STJ detectors and the outermost IR-blocking window to  $\sim 8$  mm in order to increase the solid-angle coverage to  $\Omega/4\pi \approx 10^{-3}$  (Fig. 1). The transmission of the three Al(20 nm)–parylene(100 nm) windows and the absorption of the Nb electrodes determines the quantum efficiency of the instrument at low energy (Fig. 2).

The X-ray induced signals are read out with separate custom-designed current-sensitive preamplifiers at room temperature, whose 2SK146 FET input stage has a voltage noise of  $0.5 \text{ nV}/\sqrt{\text{Hz}}$ . The preamplifier output signals have an amplitude of  $\sim 0.1 \text{ mV/eV}$  and a decay time of  $\sim 3 \mu\text{s}$ , and can thus be further processed with standard commercial analog or digital shaping amplifiers.

The STJ spectrometer is operated at a 12 inch diameter UHV chamber with a base pressure in the  $10^{-9}$  mbar range to minimize freeze-out of residual gases on the outer IR-blocking window. Samples are mounted on standardized Au-plated sample holders on low-outgassing carbon tape (solids or powder samples), sapphire disks (proteins) or behind silicon nitride windows (liquid samples). They are inserted through a load lock for fast turn-around. The sample stage in the UHV chamber can be moved in three dimensions and can be rotated for angle-dependent studies. It can also be cooled to  $\sim 15$  K with a He flow-cryostat to reduce radiation damage.

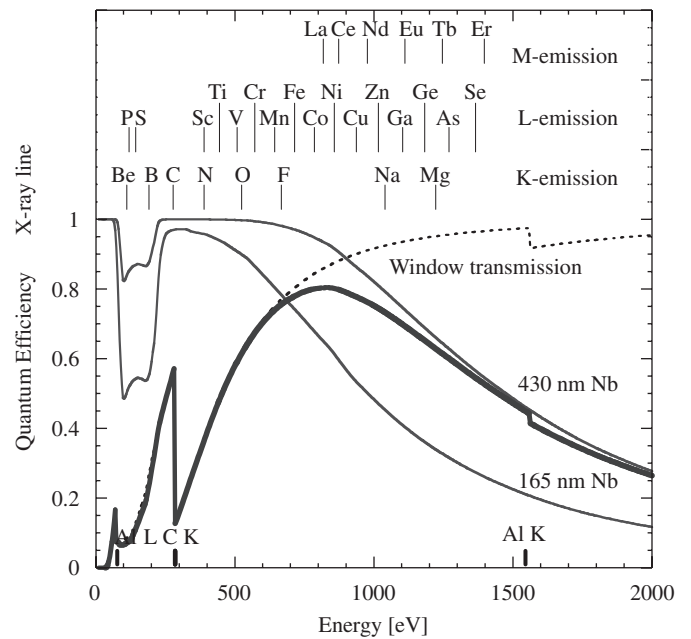


Fig. 2. The quantum efficiency of the STJ spectrometer (thick line) is set by the absorption of its Nb electrodes at high energy (thin lines) and by the IR window transmission (dotted line) at low energies. Characteristic X-ray energies of some elements of interest are listed on top.

### 3. Spectrometer performance

The spectrometer has an energy resolution between 10 and 20 eV FWHM for X-ray energies below 1 keV [2]. While smaller STJ pixels have an even higher energy

resolution [4], it is advantageous for fluorescence-detected XAS to trade off some energy resolution for higher solid angle coverage, because X-ray emission lines are rarely spaced closer than 50 eV, even in the soft X-ray band. The spectrometer sensitivity is almost never limited by line overlap, but it can be reduced by a broad spectral background, either due to pile-up or due to contamination of the detector surface. We emphasize that, in contrast to Si(Li) or Ge detectors, there is no unavoidable dead layer in STJ detectors since no electrode must be deposited on the absorbing surface. Each pixel can be operated at  $\sim 30,000$  counts/s for a total maximum count rate of  $\sim 10^6$  counts/s. In practice, the spectrometer is rarely operated much above 200,000 counts/s, even at an undulator beam line on a third generation synchrotron, because of the small pixel size and the low fluorescence yield  $\varepsilon < 10^{-3}$  for soft X-rays.

The STJ spectrometer is operated at the ABEX user facility at the undulator beam line 4.0.2 of the ALS [5]. It is primarily used for XAS on proteins, biogeochemical samples and novel materials, with typical sample concentrations of  $\sim 100$  to several  $\sim 1000$  ppm. The exact spectrometer sensitivity varies depending on the fluorescence yield  $\varepsilon$  of the element under investigation [1,6], but for a sample with a concentration  $c$  of this element, it can roughly be estimated from the signal rate  $I_S \approx I_0 \times \varepsilon \times c \times \text{QE} \times \Omega/4\pi$ , where QE is the quantum efficiency according to Fig. 2. For an incident flux  $I_0 \approx 10^{12}$  photons/s, a sample concentration  $c \approx 1000$  ppm and a fluorescence yield  $\varepsilon \approx 10^{-3}$ , about 1000–10000 signal counts can be acquired in a scan with a acquisition time of 10 s per energy step. Ideally, this would result in a statistics-limited  $S/N$  ratio of  $\sim 30$ – $100$  for a typical 1 h scan. In practice, the  $S/N$  ratio can be a factor  $\sim 2$  lower because of the small non-Gaussian component in the response function [2]. Several scans can be averaged for higher  $S/N$  ratio, especially in radiation sensitive samples where the exposure of each sample spot must be limited.

As an example, Fig. 3 shows X-ray absorption spectra at the sulfur  $L$ -edges, taken simultaneously by total electron yield (TEY) with a channeltron and by partial fluorescence yield (PFY) with the STJ spectrometer. It illustrates the sensitivity of soft X-ray XAS for chemical analysis, one of the drivers behind STJ development, since the natural linewidths of the low-energy  $L_2$  and  $L_3$  edges are very narrow compared to the observed chemical shifts of about 1 eV per oxidation state. The chemical information content is illustrated by the  $\text{Na}_2\text{MoS}_4$  data, where the  $L_2$  and  $L_3$  edges are further split by the 0.9 eV Mo 4d ligand field producing a classic 1:2:1 peak pattern. The spectra also show differences in chemical composition between the surface (TEY) and the bulk (PFY) of the sample, a common concern with biological or environmental samples

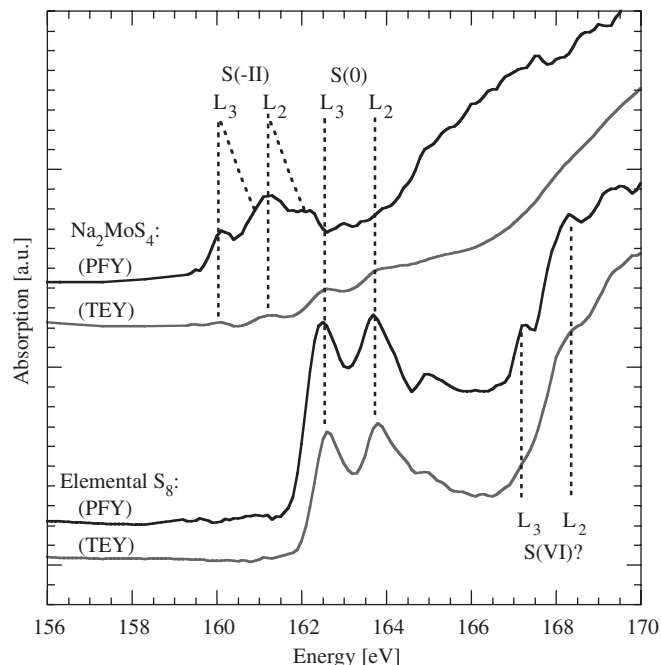


Fig. 3.  $L$ -edge spectra on sulfur model compounds, taken simultaneously by total electron yield (TEY) with a channeltron and by partial fluorescence yield (PFY) with the STJ spectrometer.

that favors XAS with photons (PFY) over electrons (TEY). On the other hand, the extremely low fluorescence yield of low-energy X-ray transitions limits the sensitivity of such measurements, in the case of sulfur  $L$ -edges to sample concentrations of several percent. As usual, the choice of the appropriate instrument therefore depends on the specific scientific question and the associated sample characteristics.

#### Acknowledgments

We thank Charles G. Young for providing the  $\text{Na}_2\text{MoS}_4$  sample, and the ALS for providing beam time. We gratefully acknowledge funding through DOE OBER, NIH Grant EB-001962 and NASA ASTID Grant NNH06AE111. This work was performed under the auspices of the US Department of Energy by University of California, Lawrence Livermore National Laboratory, under Contract no. W-7405-Eng-48.

#### References

- [1] S. Friedrich, J. Synch. Radiat. 13 (2006) 159 (review article).
- [2] S. Friedrich, et al., Nucl. Instr. and Meth. A551 (2005) 35.
- [3] S. Friedrich, et al., Nucl. Instr. and Meth. 467 (2001) 1117.
- [4] J.B. le Grand, et al., Appl. Phys. Lett. 73 (1998) 1295.
- [5] A.T. Young, et al., Nucl. Instr. and Meth. A467–A468 (2001) 549.
- [6] O.B. Drury, et al., IEEE Trans. Appl. Supercond. 15 (2005) 613.